Eur Radiol (2008) 18: 1153–1161
DOI 10.1007/s00330-008-0884-2

Angela Anjorin
Helga Schmidt
Hans-Georg Posselt
Christina Smaczny
Hanns Ackermann
Michael Deimling
Thomas J. Vogl
Nasreddin Abolmaali

Comparative evaluation of chest radiography, low-field MRI, the Shwachman-Kulczycki score and pulmonary function tests in patients with cystic fibrosis

Received: 5 March 2007
Revised: 2 January 2008
Accepted: 17 January 2008
Published online: 15 February 2008

A. Anjorin · T. J. Vogl
Institute for Diagnostic and Interventional Radiology,
Johann Wolfgang Goethe University,
Theodor-Stern-Kai 7,
D-60590 Frankfurt am Main, Germany

H. Schmidt
Department of Pediatric Radiology,
Institute for Diagnostic and Interventional Radiology,
Johann Wolfgang Goethe University,
Theodor-Stern-Kai 7,
D-60590 Frankfurt am Main, Germany

H.-G. Posselt
Clinics for Pediatry, Gastroenterology,
Johann Wolfgang Goethe University,
Theodor-Stern-Kai 7,
D-60590 Frankfurt am Main, Germany

C. Smaczny
Medical Clinics I, Pneumology,
Johann Wolfgang Goethe University,
Theodor-Stern-Kai 7,
D-60590 Frankfurt am Main, Germany

H. Ackermann
Department of Biomathematics,
Johann Wolfgang Goethe University,
Theodor-Stern-Kai 7,
D-60590 Frankfurt am Main, Germany

M. Deimling
Siemens Medical Solutions,
Karl Schall Str. 6,
D-91052 Erlangen, Germany

N. Abolmaali (✉)
OncoRay - Molecular Imaging,
Medical Faculty Carl Gustav Carus,
Dresden University of Technology,
Fetscherstraße 74, Pf 86,
D-01307 Dresden, Germany
e-mail: Nasreddin.Abolmaali@OncoRay.de
Tel.: +49-351-4587414
Fax: +49-351-449210394

Abstract The aim of this study was to investigate whether the parenchymal lung damage in patients suffering from cystic fibrosis (CF) can be equivalently quantified by the Chrispin-Norman (CN) scores determined with low-field magnetic resonance imaging (MRI) and conventional chest radiography (CXR). Both scores were correlated with pulmonary function tests (PFT) and the Shwachman-Kulczycki method (SKM). To evaluate the comparability of MRI and CXR for different states of the disease, all scores were applied to patients divided into three age groups. Seventy-three CF patients (mean SKM score: 62±8) with a median age (range) of 14 years (7–32) were included. The mean CN scores determined with both imaging methods were comparable (CXR: 12.1±4.7; MRI: 12.0±4.5) and showed high correlation ($P<0.05$, $R=0.97$). Only weak correlations were found between imaging, PFT, and SKM. Both imaging modalities revealed significantly more severe disease expression with age, while PFT and SKM failed to detect early signs of disease. We conclude that imaging of the lung in CF patients is capable of detecting subtle and early parenchymal destruction before lung function or clinical scoring is affected. Furthermore, low-field MRI revealed high consistency with chest radiography and may be used for a thorough follow-up while avoiding radiation exposure.

Keywords Thoracic radiography · Magnetic resonance imaging · Lung · Comparative study · Cystic fibrosis

Introduction

Cystic fibrosis (CF) is an autosomal recessive inherited disease that affects the chloride-ion channel of secreting tissues. Despite improved survival rates due to recent therapeutic advances [1], pulmonary failure remains responsible for up to 95% of deaths in CF patients [2, 3]. Consequently, the early assessment of pulmonary status is essential as therapy and prophylaxis are intensified with disease progression, e.g., a chronic suppressive antibiotic therapy might be indicated [4]. An array of diagnostic procedures has been established involving clinical, functional, and radiological evaluations. Among imaging techniques, conventional chest radiography (CXR) has

been used for many years to assess the extent of lung injury, and radiological scoring systems have been useful for clinical studies [5–7].

Improvements in magnetic resonance imaging (MRI) techniques have substantially increased the potential of this tool in the evaluation of the lung parenchyma [8, 9]. Standard spin-echo imaging gives limited diagnostic information in the lung with almost no signal from air-filled parenchyma [10]. MRI employing sequences with shorter TE [11, 12] allow improved signal from lung parenchyma. Many studies have been carried out in high-field systems. However, it has been shown that, when using a low-field strength of 0.2 Tesla, the T2* decay is significantly slower than with imaging at 1.5 Tesla [13]. Various authors [14–16] have proposed different sequences at 0.2 Tesla for lung imaging. When compared with true FISP imaging (fast imaging in steady-state precession) [17], the CISS (constructive interference in steady-state precession) sequence proved slightly more advantageous with respect to pixel resolution and the detection of lung pathology. The specific features of the CISS pulse sequence are the major reasons for this benefit. In addition, chronically ill CF patients appear to prefer examinations in open MRI scanners.

The aim of this study was to assess the correlation of pulmonary scoring obtained by CXR in CF patients as compared with the pulmonary scoring obtained with low-field MRI. Scoring was done using the Chrispin-Norman (CN) system applied to both modalities in patients with different duration of disease. Our hypothesis was that low-field MRI using the CISS technique is equivalent to CXR for the quantification of parenchymal pathologies of the lung. Additionally, the imaging scores were compared with nonimaging clinical evaluation methods, including pulmonary function tests (PFT) and clinical scores obtained with the Shwachman-Kulczycki [18] method.

Methods and materials

Patients

Seventy-three patients (35 females, 38 males) with varying disease severity and a median age (range) of 14 (7–32) years were examined. The minimum age of patients included in this study was set at 6 years to facilitate and guarantee compliance with the breathing orders issued during the MRI examination. To assess the results of the MRI with the progression of disease, patients were arbitrarily divided into three groups with equidistant mean ages and of approximately the same size:

Group 1 (age range 6–12 years, mean age 10 years, n=24, 9 females, 15 males), group 2 (age range 13–15 years, mean age 14 years, n=22, 14 females, 8 males), and group 3 (age above 15 years, mean age 18.4 years, n=27, 12 females, 15 males). Further divisions would not have been favorable since group sizes would have been too small to derive reliable statistical results.

Clinical assessment in all patients included measurements of the residual volumes, the forced vital capacity (FVC), and the forced expiratory volume in 1 s (FEV_1); the latter two are given as a percent of the predicted value. The clinical status was assessed by CF-experienced pediatricians and pulmonologists independent of imaging, using the Shwachman-Kulczycki scoring system [18].

This study was approved by the local ethics committee, and written informed consent was obtained from parents and patients.

Imaging

In addition to the clinically indicated CXR (posterior-anterior and lateral projections), the lungs of the patients were examined in a low-field MRI unit (Magnetom Open Viva, Siemens, Erlangen, Germany) at 0.2 Tesla utilizing the maximum performance of the 15 mT/m gradient system. Patients were examined in inspiration with a T2-weighted, two-dimensional breath-hold CISS sequence [19]. The applied sequence parameters were as follows: TR = 6 ms, TE = 3 ms, flip angle = 70°, distance factor 10%, slice thickness 20 mm, FOV = 450 mm, matrix: 256 × 256, pixel size: 2.28×1.76 mm^2, acquisition time = 5 s/slice. The acquisition time was adapted to the comfortable breath-hold time in every patient and was usually 10 s. During multiple breath-holds axial and coronal images covered the entire thorax of every patient. Additionally, three sagittal slices were acquired as follows: through the thoracic spine and through the center of the right and left lung. Neither cardiac nor respiratory gating was employed.

Imaging analysis

Two experienced pediatric radiologists (SH, AN) evaluated all images in consensus. CN scores acquired with CXR images were determined independently from the scores for the MRI images, and the readers were blinded to the patients' history. For comparison with CXR imaging, only the coronal images were analyzed to quantify parenchymal alterations. The well-known categories from CXR, i.e., bronchial line shadows, nodular/mottled shadows, ring shadows, and large shadows were translated into bronchial lines, nodules, rings, and confluent infiltrations on MRI. To generate the CN score from each quadrant, the information for all coronal images from the particular quadrant was summarized virtually. This artificial reduction of the MRI information was needed to enable the quantitative comparison of CN scores generated with CXR and MRI. The sagittal images were exclusively analyzed to quantify changes related to overexpansion including sternal bowing, kyphosis, and phrenoptosis. The extent of alterations of the

lung parenchyma and the amount of overexpansion were categorized as is done using CXR and summarized accordingly. The CN scores from both methods were scaled in three levels to represent the severity of disease (a CN score under 10 = mild, a score between 10 and 20 = moderate and above 20 = severe). For clinical reporting, the CXR scores were used, and additional findings from MRI, including the analysis of the axial images, were mentioned.

Statistics

Statistical analysis was performed with the BiAS statistical software package (Version 8.2, http://www.bias-online.de). The agreement between MRI and CXR scores was assessed using the method of Bland and Altman [20]. The Passing-Bablok regression [21] tested the equality of measurement between MRI and CXR findings. The Wilcoxon matched-pairs test assessed the difference between the CN scores of both imaging modalities for each patient. Spearman-Rank correlation was used to calculate the correlation between CXR and MRI findings as well as with the PFT and clinical scores within each age group. Statistical significance was assumed if the null hypothesis could be rejected at the $P=0.05$ level.

Results

Image analysis

MRI of the lung parenchyma was possible in all subjects. The door-to-door time for the MRI examination was 15–20 min. The mean ± standard deviation total score for the MR images for all age groups was 12.0±4.5, with a higher score than CXR in 23 patients (31.5%). The overall CN score of the CXR for all age groups was 12.1±4.7 with a higher score than MRI in 25 patients (34.3%). Descriptive statistics are given in Table 1. There was a highly significant correlation between CXR and MRI scores (Fig. 1) for all the matched pairs ($P<0.05$, $R=0.97$). The difference in the CN scores determined with both methods was 0.12 and revealed no significant difference. The twofold standard deviation of the difference was 2.28. Figure 2 shows the correlation among the CN scores using the Bland-Altman method. The Passing-Bablok regression showed a significant correlation ($P<0.05$, $R=0.96$) between the CN scores of MRI and CXR. According to the Wilcoxon matched-pairs test, the CN scores for CXR and MRI were not significantly different ($P=0.46$).

The Spearman-Rank correlation coefficients between CXR-CN and MRI-CN scores, pulmonary function test results, and clinical scores are summarized in Table 2. The correlation between the CN scores for CXR and MRI was very high. Overall, CXR-CN and MRI-CN scores correlated better with the measured FEV_1 than with FVC. Both CXR-CN and MRI-CN scores correlated to some degree with the Shwachman-Kulczycki scores. The different categories of the CN score were classified by CXR and MRI as follows:

- Scores for thoracic deformation (sternal bowing, spinal kyphosis) and for the diaphragm position were identical for every patient in both modalities.
- Identification of interstitial lines and large shadows was nearly identical for both imaging techniques. The maximum difference was 1.
- Differences occurred for the detection of rings and mottled shadows. Rings were identified more frequently on CXR than on MRI. Conversely, mottled shadows were detected more frequently on MRI (Fig. 3).

Imaging CN scores as a function of age

Results of PFT and clinical scoring in each of the three age groups are summarized in Table 3. In all patients, PFT confirmed a general pattern of obstructive lung disease

Table 1 Descriptive statistics of the CN scores (CXR and MRI) with respect to three age groups

CN score (maximum score 38)		6–12 years	13–15 years	>15 years	All age groups
CXR	Maximum	15	22	25	25
	Minimum	2	6	3	2
	Median	7.5	11	15	11
	Mean ± SD	8.6±3.0	11.8±3.5	16.0±5.1	12.1±4.7
MRI	Maximum	17	23	24	24
	Minimum	3	6	2	2
	Median	7.5	11	17	11
	Mean ± SD	8.8±3.4	11.5±3.3	15.6±4.6	12.0±4.5

CN Chrispin-Norman, *CXR* Conventional chest radiography, *MRI* magnetic resonance imaging

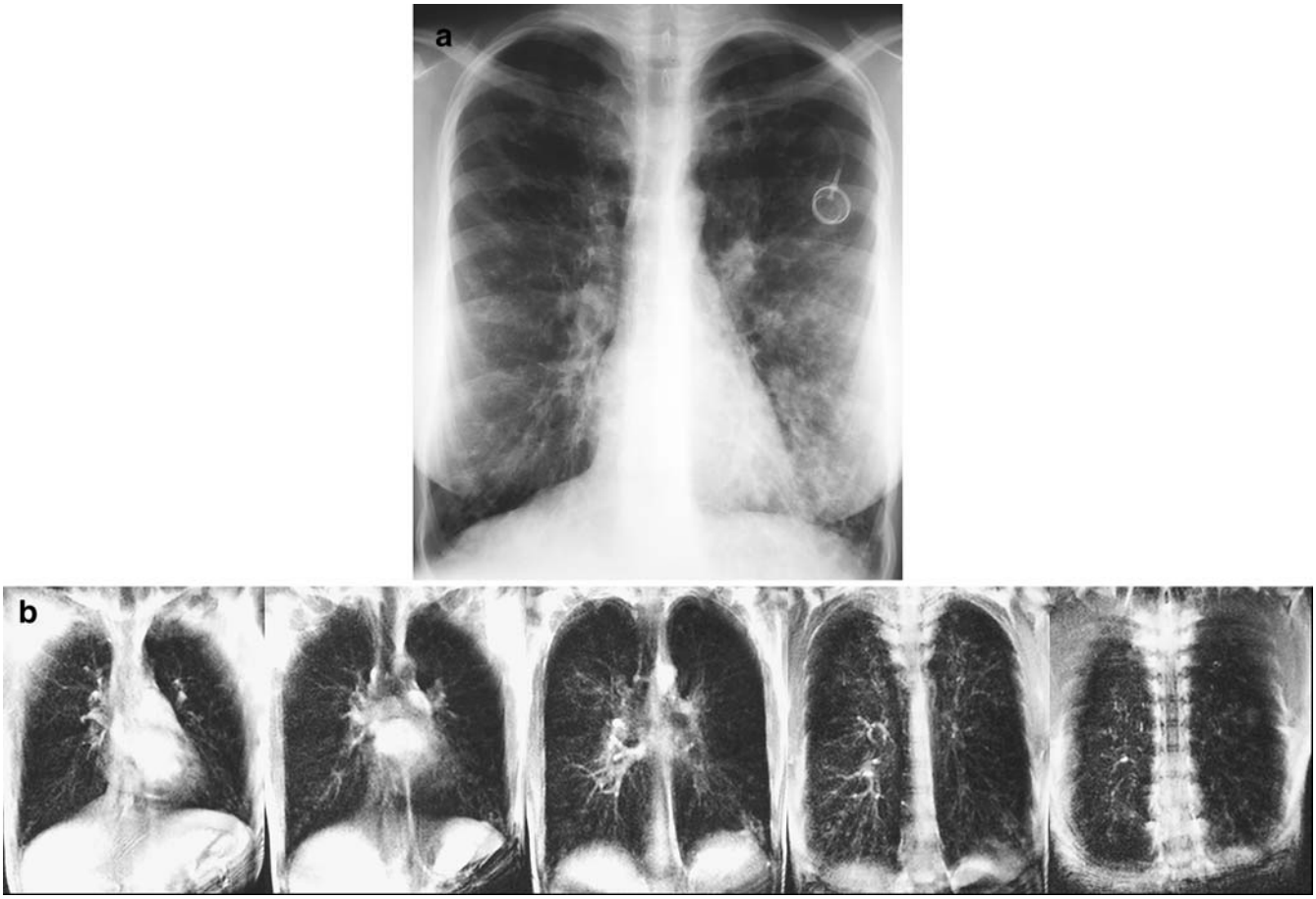

Fig. 1 **a** Chest radiography (posteroanterior) of a 15-year-old female patient (Shwachman-Kulczycki score: 45, FEV_1: 30%, FVC: 39%) showing diffuse changes in the lung parenchyma with mottled shadows and bronchiectases particularly in the left lower quadrant. Signs of emphysema are visible. CN score from CXR was 21. **b** Coronal MR images of the thorax of the same patient (CISS, slice thickness: 20 mm) revealing signs of emphysema, bronchiectases, diffuse mottled shadows and scars. CN score from MRI was 21

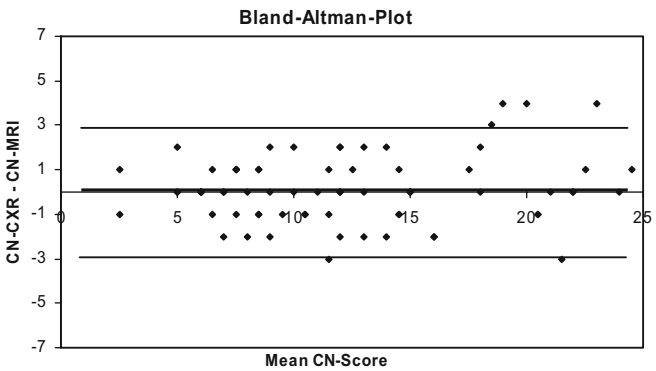

Fig. 2 Graph showing the Bland-Altman analysis of the CN scores as determined by CXR and MRI. The mean difference is 0.1 (*thick line*), the *thin lines* represent the twofold standard deviation. The data points for the *x-axis* arise from the mean CN value that was calculated using the results of CXR and MRI. The number of data points is lower than the number of patients in this study since some patients had identical pairs of variates

with decreased expiratory volumes and flow rates and increased residual volumes. In general, PFT, especially for FVC, could not demonstrate significant changes between groups 1 and 2. The mean overall Shwachman-Kulczycki clinical score was 62±8. Of note, this clinical scoring system failed to demonstrate any differences between groups 1 and 2; both age groups had mean scores of approximately 63. For both the PFT and the Shwachman-Kulczycki scores, a statistically significant ($P<0.05$) increase was observed for patients 15 years and older (group 3).

Table 1 summarizes the CN scores for both imaging modalities in each of the three age groups. The mean CN scores for both imaging modalities were similar in the different age groups showing increasing CN scores with increasing age. The correlation coefficient between the two methods was significant in all groups ($P<0.05$; $R=0.94$ in group 1, $R=0.93$ in group 2, $R=0.97$ in group 3).

Figures 4 and 5 show the distribution of the three levels of disease severity within each age group for MRI and CXR respectively. The distribution of disease severity in

Table 2 Spearman correlation coefficients between total CN scores from both CXR and MRI, Shwachman-Kulczycki scores, and pulmonary function test results

Correlation between	*R*	*P*
CXR and Shwachman-Kulczycki	–0.52	<0.001
MRI and Shwachman-Kulczycki	–0.53	<0.001
CXR and FEV_1	–0.65	<0.001
MRI and FEV_1	–0.65	<0.001
CXR and FVC	–0.46	<0.001
MRI and FVC	–0.47	<0.001
CXR and MRI	0.97	<0.001

CXR Conventional chest radiography, *MRI* magnetic resonance imaging, *FEV_1* forced expiratory volume in 1 s, *FVC* forced vital capacity

groups 1 and 3 was similar for both imaging modalities. In group 2, 62.5% patients were classified as having mild disease on MRI and 58% on CXR. Moderate disease was the classification in 12.5% (MRI) and 25% (CXR) of the patients. Finally, 25% (MRI) and 12% (CXR) were classified as having severe disease.

Discussion

Patients with CF experience chronic lung disease caused by repeated infections. Although chest radiographs can detect early changes in the airways, cross-sectional imaging provides additional information. Computed tomography (CT) is the standard of reference for imaging of the lung, but the inherent risk due to ionizing radiation is not negligible. This is of particular importance in young patients with comparatively high radiosensitivity and long follow-up periods involving frequent imaging. The lifetime mortality risk resulting from stochastic effects has been estimated by age- and gender-dependent risk factors from the multiplicative model recommended in the ICRP 60 publication as 16%/Sv for girls and 13%/Sv for boys 10 years of age [22].

To avoid radiation exposure, MRI may be performed. With respect to non-contrast-enhanced proton-based morphological MRI of the lung parenchyma, two different approaches can be identified. The first utilizes high-field imaging above 1 Tesla [23, 24] with thin slices from 3 to 8 mm. Herein, susceptibility artifacts are reduced by fast imaging at short TE and parallel acquisition techniques. This method strives to compete with CT. In the second approach, low-field imaging is performed at or below 0.5 Tesla in which susceptibility artifacts are within acceptable ranges due to the lower field strength. The limited signal-to-noise ratio is balanced by thicker slices of up to 55 mm [16]. Since the information contained in thick slices is averaged into one image, this technique is, to a certain extent, more comparable with radiography, where all the information is averaged into one image. In comparison with high-field MRI systems, this appears to be a disadvantage since resolution is lower. But as shown in our work, for CN scoring, the spatial resolution is sufficient. For imaging of the lung parenchyma at 0.2 Tesla, different sequence techniques have been compared [17], including the CISS sequence [19]. This MRI technique is easy to perform and comparatively fast. No

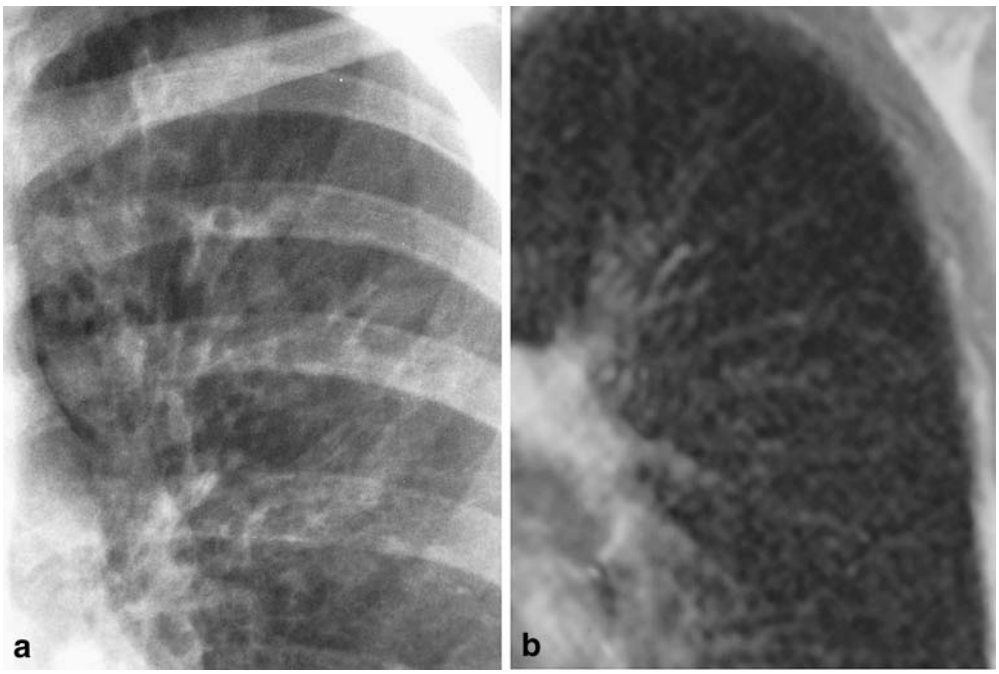

Fig. 3 **a** Detail magnification of a chest radiography (posteroanterior) of a 13-year-old male patient (Shwachman-Kulczycki score: 70, FEV_1: 82%, FVC: 86%) showing at least two larger ring shadows in the upper left quadrant. Total CN score from CXR was 9. **b** Detail magnification of one of the coronal MR images of the thorax (acting as a representative) from the same patient. There are two ring shadows in the upper part of the image, not corresponding to the ring shadows in **a**. Total CN score from MRI was 10

Table 3 Results of the pulmonary function tests and the Shwachman-Kulczycki scores in three age groups

Parameter		6–12 years	13–15 years	Above 15 years
FEV_1	Maximum	114	128	110
	Minimum	57	30.2	20
	Median	84.5	83.5	67
	Mean ± SD	87.2±13.6	83.6±15.8	65.2±20.0
FVC	Maximum	107	114	108
	Minimum	63.6	39.3	30
	Median	85	84	81.5
	Mean±SD	85.8±9.4	85.3±14.2	75.9±15.9
Shwachman-Kulczycki score	Maximum	70	75	75
	Minimum	45	35	35
	Median	65	65	60
	Mean±SD	64.4±5.1	63.2±7.0	58.9±10.3

modifications of the scanner hardware or the software are needed; the sequence can easily be adapted with the user platform.

In this study, we compared the visualization of CF-based pulmonary pathology as assessed with MRI with the commonly used imaging modality for follow-up in CF, namely CXR. Since pulmonary alteration in CF increases with age, this comparison was done in different age groups. We included patients who were at least six years of age, since young patients only very rarely receive continuous pulmonary imaging for the follow-up of chronic CF-related pulmonary damage. Additionally, pulmonary function tests and clinical scoring were compared with the imaging findings.

The comparability of the MRI and CXR images was assessed using a quantitative scoring system. We decided to use the Chrispin-Norman chest radiograph scoring system

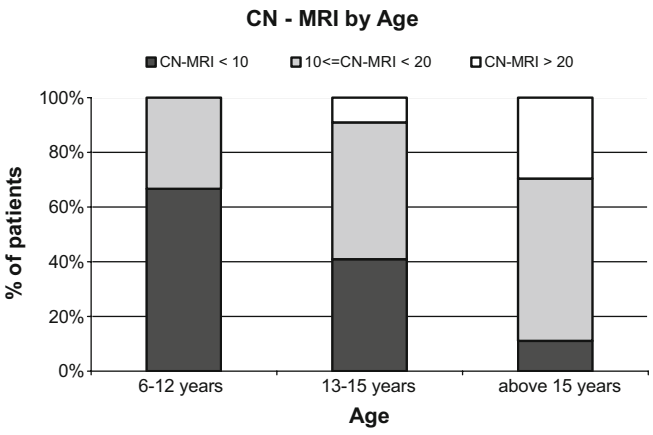

Fig. 4 The severity of disease as shown by the MRI-CN score among the three age groups

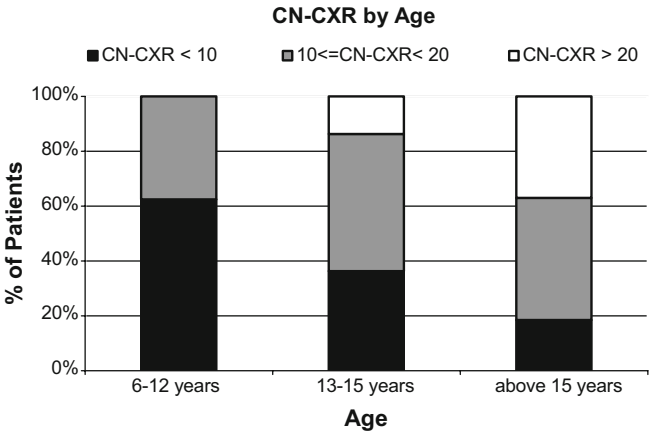

Fig. 5 The severity of disease as shown by the CXR-CN score among the three age groups

[6] because it was developed for children, has a low interobserver variability [25], and the pathologic findings listed within this scoring system can be detected on CXR as well as on MRI scans [26]. One limitation of the comparative CN-score evaluation of CXR and MRI, however, is the need to average the CN score of MRI in every lung quadrant in several coronal slices. This limitation is inherent in every investigation comparing a projection technique with a cross-sectional method. In our evaluation we therefore had to "worsen" the results of the MRI, losing the additional spatial information of the cross-sectional images. Obviously, this shortcoming exclusively affects the quantitative comparison in the study. For individual patient care, additional spatial information is provided by MRI and may be applied in clinical practice. Since CXR is a broadly applied tool for the follow up of CF patients, we decided to use this technique for our comparison. Nevertheless, CXR is a rough tool itself, especially for the evaluation of subtle, i.e., early alterations of the lung. Recent dose-saving techniques for multislice CT (MSCT) applications will, by far, provide more detailed information on the pulmonary parenchyma and will exceed the information that can be acquired with low-field MRI. However, neither MSCT nor high-field MRI have found their way to clinical application in the annual follow-up of CF patients.

The patients in this study had a broad spectrum of CN scores (2–25) on CXR, and those determined by MRI were similar. The scores for thoracic deformation and diaphragm dome position were identical for both techniques used. The latter compares well with the inspiratory image acquisition utilized by both modalities. Minor differences (maximum CN-score difference = 1) were found for the identification of large shadows and bronchial lines. The latter finding indicates that the spatial resolution of the CISS technique at a slice thickness of 20 mm applied to the lung parenchyma is sufficient to visualize CF-related pathologies. Occasionally, large shadows detected on CXR were identified as

several mottled shadows on MRI. More frequently, differences occurred in the detection of rings and mottled shadows. Rings were identified more frequently on CXR. The loss of information on rings in MRI can be explained by the comparatively large slice thickness since the wall of the structure generating a ring in CXR is thin (e.g., 2 mm) as compared to the adjacent air space (e.g. 18 mm) at a slice thickness of 20 mm in low-field MRI. Mottled shadows, however, were more frequently detected on MRI, most probably due to the higher content of protons in filled (fluid or infiltration) air spaces. This result might be related to the fact that CXR is a projection technique. Therefore, subtle mottled shadows may not have been visible on CXR. Nevertheless, both imaging scores showed a highly significant correlation for all the matched pairs ($P<0.05$, $R=0.97$). The difference in the CN scores determined with both methods was 0.12 and was not significant. The Passing-Bablok regression showed a significant correlation ($P<0.05$, $R=0.96$) between the CN scores of MRI and CXR. According to the Wilcoxon matched-pairs test, the CN scores for CXR and MRI were not significantly different ($P=0.46$).

While the CN score allows the quantification of parenchymal damage, three typical CF-related findings are described in the CN system but not quantified: signs of pneumonia, lymph nodes, and pleural thickening. In all of our patients, the findings in the first category matched completely between MRI and CXR, but for the latter two categories MRI detected, as expected, many more lesions than CXR. This information might be important, for example in patients scheduled for lung transplantation with widespread pleural thickening. Furthermore, as previously reported [23, 26], a number of additional findings may be provided by MRI data. These may or may not be related to CF. As mentioned above, typical CF-related findings that will be detected by MRI with higher sensitivity than by CXR are mediastinal lymph nodes, pleural thickening, and pneumonia. Non-CF-related findings that will be visualized by MRI with high sensitivity are tumors and pulmonary nodules, cysts (e.g., bronchogenic cysts), and congenital pulmonary malformations. Anomalies of the thoracic wall, namely the ribs, and of the vertebral column are detected as well. Using nontriggered low-field MRI, certain congenital cardiac malformations and major vascular malformations will be visualized sufficiently. Frequently, large parts of the upper abdomen are visualized and hepatocirrhosis or pancreatic atrophy may be detected. The number of extra-thoracic findings discovered by MRI will vary with the indication, and a thorough follow-up will allow early detection of such pathologies.

As anticipated, all observed scores worsened with patient age, and PFT confirmed obstructive lung disease in all patients. However, the PFT and the Shwachman-Kulczycki score failed to demonstrate significant changes between the two younger patient groups. This might be related to both limited sensitivity of administered techniques and questionable cooperation of younger children [27]. A significant increase in the clinical scores was found only for the older patient groups.

The coefficients of the correlations between MRI and CXR scores with the PFT were significant but low. A considerable consistency was not identified between either the clinical and MRI or clinical and CXR scores. Similar findings are reported when using CT [28]. In our opinion, the lack of relationship between clinical scores and PFT, as compared to imaging scores, can be explained by the sensitive and early detection of the morphological destruction of the lung parenchyma in CF, which anticipates the decline of the other tests by far. Furthermore, the confidence intervals of individual measurements of the function tests are wide, especially in very young children, who do not cooperate well during such tests [27]. As evidenced by our results, there is a poor correlation between MRI scores, PFT (especially FVC), and clinical scores. Matthews et al. [29] demonstrated how chest radiographic scores and respiratory function tests in children with cystic fibrosis increased with age.

The utility of lateral CXR films for the acquisition of the CN score has been questioned [30]. In some institutes, in an attempt to minimize radiation exposure, CF follow-up is performed without such films. Conversely, CT has been advocated for the follow-up of children with CF [31]. As shown in this study, the major advantage would be the earlier detection of asymptomatic, but clinically relevant, bronchiectases, especially in the lower lobes. Although low-dose CT techniques would reduce radiation exposure in children, the validity of such an imaging technique is limited [32]. As with low-dose CT, the detection of subtle bronchiectases might be difficult with low-field MRI due to the comparatively large slice thickness. A larger comparative study in CF patients using CT and low-field MRI is not available [33]. To detect such early findings in children, high-field MRI might be a reasonable alternative [34]. At present, the follow-up of parenchymal, i.e., structural changes in the lung of patients suffering from CF is feasible with MRI at any field strength. The decision to use a high-field rather than a low-field MRI is mainly based on availability and is dependent on a cost-benefit analysis.

The major advantage of high-field MRI is the possibility to assess structural information together with functional information, e.g., local ventilation, in one examination [16, 35], thereby reducing imaging costs and increasing patient compliance. In two recent studies, hyperpolarized 3-helium MRI has been successfully investigated in comparison with PFT in children [36] and in comparison with spirometry and high-resolution CT in adults [37]. These observers emphasize the growing potential of MRI to visualize functional parameters.

An advantage of low-field MRI is the availability of the "open" design of the magnets with better patient accessibility and fewer terminations of examinations, especially in claustrophobic patients. Furthermore, pur-

chase and running costs of these systems are noticeably lower than for high-field scanners.

Considering these facts, what could be the possible clinical conclusion? The radiation delivered to the patients for follow-up with CXR is small, even over years; nevertheless, the consequences of this radiation are not predictable in an individual patient. With respect to continuous improvement of therapeutic strategies, life expectancy is likely to increase further, and longer follow-up, i.e., even higher doses of radiation, can be expected. Therefore, dose reduction in diagnostic imaging remains a matter of continuing debate. New and possibly expensive therapies with high specificity and probable toxicity rely on the early diagnosis of disease progression. Consequently, the sensitivity of imaging and the accuracy of the diagnostic conclusion have to be improved.

Does the diagnostic equality between CXR and low-field MRI of the lung parenchyma, as shown in this study, provide a reason to conduct the more expensive and somewhat time-consuming cross-sectional technique? According to our experience and other research, the major clinical benefit results from additional findings detected with MRI that were not detectable with CXR. In our opinion, this benefit justifies the higher strain for the patients, and also the higher costs of the diagnostic procedure. Years ago, this question encouraged research for further development of advanced imaging techniques with higher resolution at decreasing doses (MSCT) and zero radiation burden at comparable spatial resolution (high-field MRI). Moreover, functional MRI of the lung parenchyma can be expected to add significant additional value to the diagnostic toolbox. Comprehensive imaging with high sensitivity will allow for a timely and early onset of specific therapy and will presumably improve life expectancy and quality of life of CF patients.

The ongoing advances in MRI techniques to assess morphological and functional changes of the lung parenchyma and pulmonary circulation in CF patients will increase the acceptance of MRI by pediatricians and pulmonologists. As demonstrated, low-field MRI is suitable to assess the CN score in CF patients and may even provide additional information (Fig. 1). It is therefore a valuable supplement for the examination of CF patients.

Conclusion

Low-field MRI of the thorax provides considerable information about the lung parenchyma in cystic fibrosis that is comparable to the findings from conventional CXR. Beyond this, MRI provides additional information on pleural, mediastinal, and extrathoracic findings not available in CXR. The suggested MRI technique using the CISS sequence is able to add valuable diagnostic information in patients with CF.

Acknowledgements Nasreddin Abolmaali is kindly sponsored by the "Bundesministerium für Bildung und Forschung," BMBF Contract 03ZIK042.

References

1. Rosenecker J, Huth S, Rudolph C (2006) Gene therapy for cystic fibrosis lung disease: current status and future perspectives. Curr Opin Mol Ther 8:439–445
2. Wiedemann B, Steinkamp G, Sens B, Stern M (2001) The German cystic fibrosis quality assurance project: clinical features in children and adults. Eur Respir J 17:1187–1194
3. Ruzal-Shapiro C (1998) Cystic fibrosis. An overview. Radiol Clin North Am 36:143–61
4. Yankaskas JR, Marshall BC, Sufian B, Simon RH, Rodman D (2004) Cystic fibrosis adult care: consensus conference report. Chest 125:1S–39S
5. Brasfield D, Hicks G, Soong S, Peters J, Tiller R (1980) Evaluation of scoring system of the chest radiograph in cystic fibrosis: a collaborative study. AJR Am J Roentgenol 134:1195–1198
6. Chrispin AR, Norman AP (1974) The systematic evaluation of the chest radiograph with cystic fibrosis. Pediatr Radiol 2:101–105
7. Conway SP, Pond MN, Bowler I, Smith DL, Simmonds EJ, Joanes DN, Hambleton G, Hiller EJ, Stableforth DE, Weller P et al (1994) The chest radiograph in cystic fibrosis: a new scoring system compared with the Chrispin-Norman and Brasfield scores. Thorax 49:860–862
8. Kauczor HU, Kreitner KF (1999) MRI of the pulmonary parenchyma. Eur Radiol 9:1755–1764
9. Ley S, Puderbach M, Fink C, Eichinger M, Plathow C, Teiner S, Wiebel M, Müller FM, Kauczor HU (2005) Assessment of hemodynamic changes in the systemic and pulmonary arterial circulation in patients with cystic fibrosis using phase-contrast MRI. Eur Radiol 15:1575–1580
10. Gamsu G, Sostman D (1989) Magnetic resonance imaging of the thorax. Am Rev Respir Dis 139:254–274
11. Mayo JR, MacKay A, Muller NL (1992) MR imaging of the lungs: value of short TE spin-echo pulse sequences. AJR Am J Roentgenol 159:951–956
12. Muller CJ, Loffler R, Deimling M, Peller M, Reiser M (2001) MR lung imaging at 0.2 T with T1-weighted true FISP: native and oxygen-enhanced. J Magn Reson Imaging 14:164–168
13. Deimling M (2000) True FISP imaging of lung parenchyma at 0.2 Tesla. Proc Int Soc Mag Reson Med 8:2202
14. Martirosian P, Boss A, Fenchel M, Deimling M, Schafer J, Claussen CD, Schick F (2006) Quantitative lung perfusion mapping at 0.2 T using FAIR true-FISP MRI. Magn Reson Med 55:1065–1074
15. Schafer JF, Vollmar J, Schick F, Seemann MD, Mehnert F, Vonthein R, Aebert H, Claussen CD (2002) Imaging diagnosis of solitary pulmonary nodules on an open low-field MRI system–comparison of two MR sequences with spiral CT. Röfo 174:1107–1114

16. Zapke M, Topf HG, Zenker M, Kuth R, Deimling M, Kreisler P, Rauh M, Chefd'hotel C, Geiger B, Rupprecht T (2006) Magnetic resonance lung function–a breakthrough for lung imaging and functional assessment? A phantom study and clinical trial. Respir Res 7:106
17. Abolmaali ND, Schmitt J, Krauss S, Bretz F, Deimling M, Jacobi V, Vogl TJ (2004) MR imaging of lung parenchyma at 0.2 T: evaluation of imaging techniques, comparative study with chest radiography and interobserver analysis. Eur Radiol 14:703–708
18. Shwachman H, Kulczycki LL (1958) Long-term study of one hundred five patients with cystic fibrosis; studies made over a five- to fourteen-year period. AMA J Dis Child 96:6–15
19. Casselman JW, Kuhweide R, Deimling M, Ampe W, Dehaene I, Meeus L (1993) Constructive interference in steady state-3DFT MR imaging of the inner ear and cerebellopontine angle. AJNR Am J Neuroradiol 14:47–57
20. Bland JM, Altman DG (1986) Statistical methods for assessing agreement between two methods of clinical measurement. Lancet 1:307–310
21. Passing H, Bablock W (1983) A new biometrical procedure for testing the equality of measurements from two different analytical methods. J Clin Chem Clin Biochem 21:709–720
22. ICRP (1991) ICRP publication 60: 1990 recommendations of the International Commission on Radiological Protection edn. Elsevier, Amsterdam
23. Hebestreit A, Schultz G, Trusen A, Hebestreit H (2004) Follow-up of acute pulmonary complications in cystic fibrosis by magnetic resonance imaging: a pilot study. Acta Paediatr 93:414–416
24. Eichinger M, Puderbach M, Heussel CP, Kauczor HU (2006) MRI in mucoviscidosis (cystic fibrosis). Radiologe 46:275–281
25. Terheggen-Lagro S, Truijens N, van Poppel N, Gulmans V, van der Laag J, van der Ent C (2003) Correlation of six different cystic fibrosis chest radiograph scoring systems with clinical parameters. Pediatr Pulmonol 35:441–445
26. Wagner M, Bowing B, Kuth R, Deimling M, Rascher W, Rupprecht T (2001) Low field thoracic MRI–a fast and radiation free routine imaging modality in children. Magn Reson Imaging 19:975–983
27. Cooper PJ, Robertson CF, Hudson IL, Phelan PD (1990) Variability of pulmonary function tests in cystic fibrosis. Pediatr Pulmonol 8:16–22
28. Brody AS, Klein JS, Molina PL, Quan J, Bean JA, Wilmott RW (2004) High-resolution computed tomography in young patients with cystic fibrosis: distribution of abnormalities and correlation with pulmonary function tests. J Pediatr 145:323–8
29. Matthews DJ, Warner JO, Chrispin AR, Norman AP (1977) The relationship between chest radiographic scores and respiratory function tests in children with cystic fibrosis. Pediatr Radiol 5:198–200
30. Benden C, Wallis C, Owens CM, Ridout DA, Dinwiddie R (2005) The Chrispin-Norman score in cystic fibrosis: doing away with the lateral view. Eur Respir J 26:894–897
31. de Jong PA, Nakano Y, Lequin MH, Mayo JR, Woods R, Pare PD, Tiddens HA (2004) Progressive damage on high resolution computed tomography despite stable lung function in cystic fibrosis. Eur Respir J 23:93–97
32. de Jong PA, Nakano Y, Lequin MH, Tiddens HA (2006) Dose reduction for CT in children with cystic fibrosis: is it feasible to reduce the number of images per scan? Pediatr Radiol 36:50–53
33. Abolmaali N, Schmidt H, Anjorin A, Posselt H-G, Vogl TJ (2002) Chrispin-Norman-score and Bhalla-score of patients with cystic fibrosis: comparative study of chest radiographs and MR-imaging. Eur Radiol 12(Suppl 1):227
34. Puderbach M, Eichinger M, Gahr J, Ley S, Tuengerthal S, Schmähl A, Fink C, Plathow C, Wiebel M, Müller FM, Kauczor HU (2007) Proton MRI appearance of cystic fibrosis: comparison to CT. Eur Radiol 17:716–24
35. Altes TA, Eichinger M, Puderbach M (2007) Magnetic resonance imaging of the lung in cystic fibrosis. Proc Am Thorac Soc 4:321–327
36. van Beek EJ, Hill C, Woodhouse N, Fichele S, Fleming S, Howe B, Bott S, Wild JM, Taylor CJ (2007) Assessment of lung disease in children with cystic fibrosis using hyperpolarized 3-helium MRI: comparison with Shwachman score, Chrispin-Norman score and spirometry. Eur Radiol 17:1018–1024
37. McMahon CJ, Dodd JD, Hill C, Woodhouse N, Wild JM, Fichele S, Gallagher CG, Skehan SJ, van Beek EJ, Masterson JB (2006) Hyperpolarized 3helium magnetic resonance ventilation imaging of the lung in cystic fibrosis: comparison with high resolution CT and spirometry. Eur Radiol 16:2483–2490